Variable Modes of Nickel(II) Coordination with Macrocyclic Ligands Based on 1,5-Bis(2-mercaptoethyl)-1,5-diazacyclooctane (BME-DACO)

Marcetta Y. Darensbourg,* Ivan Font, Daniel K. Mills, Magdalena Pala, and Joseph H. Reibenspies

Department of Chemistry, Texas A&M University, College Station, Texas 77843

Received July 2, 1992

The synthesis, structural characterization, and spectroscopic and magnetic properties of the Ni^{II} complexes containing macrocyclic ligands derived from 1,5-bis(2-mercaptoethyl)-1,5-diazacyclooctane are described. The cis orientation of thiolate sulfurs rigidly held in (BME-DACO)Ni^{II} (**1**) permits high-yield template syntheses of macrocycle ligands. Thus reaction of **1** with 1,3-dibromopropane gives a four-coordinate N_2S_2Ni complex, (4,8-dithia-1,11-diazabicyclo-[9.3.3]heptadecane)nickel(II) bromide, [Ni(bicycle)]Br_2 (**3a**). Alkylation of **1** with bis(2-iodoethyl) ether results in a six-coordinate complex, containing a pentadentate, N_2S_2O donor macrocyclic ligand, (7-oxa-4,10-dithia-1,13-diazabicyclo[11.3.3]nonadecane)iodonickel(II) iodide, [(Ni(ether)I]I (**4a**). Complex **3a** crystallizes in the monoclinic $P2_1/c$ (No. 14) space group with a = 17.384 (7) Å, b = 15.529 (6) Å, c = 15.153 (4) Å, β = 104.42 (3)°, V = 3962 Å^3, and Z = 8. Complex **4b** [Ni(ether)I]BPh_4, crystallizes in the orthorhombic $P2_12_12_1$ (No. 18) space group with a = 10.016 (2) Å, b = 11.834 (3) Å, c = 30.127 (8) Å, V = 3570 (1) Å^3, and Z = 4. In pseudo-square-planar **3a** (a 2.947 (2) Å bromide interaction with Ni^{II} creates a virtual square pyramid), the metalladiazacyclohexane rings are in the chair/boat configurations. However, in pseudooctahedral **4b**, the folding back of the eight-membered NiS_2C_4O ring to accommodate Ni–O bonding and the presence of an iodide ligand trans to the oxygen enforce the uncommon chair/chair configuration of the fused metalla rings. The larger macrocycle of **4** creates a larger N_2S_2 cavity, with Ni–S distances in **4b** of 2.405 (2) and 2.362 (2) Å and in **3a** of 2.188 (3) and 2.201 (3) Å. The relative accessibility of the Ni^{I} oxidation state determined by cyclic voltammetry reflects this cavity size, with the larger yielding more positive values of the $Ni^{II/I}$ couple. Electrochemical studies of the ion-exchanged derivatives of **4** found the following dependence of the $Ni^{II/I}$ redox couple on the nature of the nickel-bound halide ligand: $E_{1/2}(I^-) > E_{1/2}(Br^-) > E_{1/2}(Cl^-)$. Factors which influence the interconversion between four- and six-coordination of **3** and **4** are explored.

Introduction

The cyclic 1,5-diazacyclooctane, DACO, ligand has been shown to strongly coordinate to metal centers in a bidentate fashion, forming square-planar four-coordinate complexes.[1-3] Of the three conformations illustrated in Chart I for metal/DACO binding, only the chair/boat form of the metalladiazacyclohexane ring has previously been observed in structural analyses. In fact, an early report[2] of the structure of $(DACO)_2Ni^{2+}$ contended that DACO was a planar eight-membered ring "folded" about the two nitrogen donors, a conclusion most certainly in error due to disorder in the central methylene group of the C_3 portion of the ring. More recently, Boeyens, Hancock, and Fox[4] repeated the structure refinement using empirical force field methods and agreed with the original assumption[1] that the metalla rings are in the boat/chair conformation. The central CH_2 group in the boat configuration sterically restricts axial ligation of the metal.

Addition of pendant arms such as $-CH_2CO_2^-$ or $-CH_2CH_2S^-$ to the DACO ring at N forms tetradentate ligands (designated DACODA and BME-DACO, respectively) that give very stable complexes with Cu^{II}, Ni^{II}, Co^{II}, Zn^{II}, Cd^{II}, and Pb^{II} ions.[5-10] The DACODA complexes of Ni^{II} and Co^{II} are pentacoordinate, square pyramidal as in the case of $[Ni(DACODA)H_2O]\cdot 2H_2O$.[6] The metalla rings are in the chair/boat arrangement, with a water molecule occupying the fifth site. The central methylene hydrogen from the boat form of a metalladiazacyclohexane ring trans to the water ligand is 2.51 (9) Å from nickel.[6] The four-coordinate (bis(mercaptoethyl)diazacyclooctane)nickel complex, (BME-DACO)Ni^{II} (**1**), shows disorder in the crystal structure resulting in an equal distribution of chair/boat and chair/chair conformers, thus disputing the rigidity expected for the metal-bound DACO ligand.[9]

Chart I

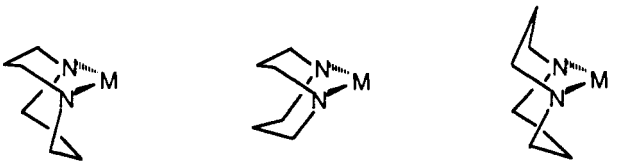

chair/boat chair/chair boat/boat

Due to the nucleophilicity of the thiolate sulfur sites in (BME-DACO)Ni^{II}, the complex has been a precursor to a broad range of derivatives modified at sulfur.[11] Alkylation with methyl iodide occurs at one or two sulfur sites, dependent on stoichiometry. With the large ZnI_4^{2-} counterion the two methyl groups are on either side of the N_2S_2Ni square plane,[11] while with iodide as counterion a long-range Ni- - -I interaction results in a syn arrangement of methyl groups (eq 1).[9]

(1) Musker, W. K.; Hussain, M. S. *Inorg. Chem.* **1966**, *5*, 1416.
(2) Royer, D. J.; Schievelbein, V. H.; Kalyanaraman, A. R.; Bertrand, J. A. *Inorg. Chim. Acta* **1972**, *6*, 307.
(3) Yamaki, S.; Fukuda, Y.; Sone, K. *Chem. Lett.* **1982**, 269.
(4) Boeyens, J. C. A.; Fox, C. C.; Hancock, R. D. *Inorg. Chim. Acta* **1984**, *87*, 1.
(5) Averill, D. F.; Legg, J. I.; Smith, D. L. *Inorg. Chem.* **1972**, *11*, 2344.
(6) (a) Nielson, D. O.; Larsen, M. L.; Willett, R. D.; Legg, J. I. *J. Am. Chem. Soc.* **1971**, *93*, 5079. (b) Legg, J. I.; Nielson, D. O.; Smith, D. L.; Larsen, M. L. *J. Am. Chem. Soc.* **1968**, *90*, 5030.
(7) Broderick, W. E.; Kanamori, K.; Willett, R. D.; Legg, J. I. *Inorg. Chem.* **1991**, *30*, 3875.
(8) Kanamori, K.; Broderick, W. E.; Jordan, R. F.; Willett, R. D.; Legg, J. I. *J. Am. Chem. Soc.* **1986**, *108*, 7122.
(9) Mills, D. K.; Reibenspies, J. H.; Darensbourg, M. Y. *Inorg. Chem.* **1990**, *29*, 4364.
(10) Hancock, R. D.; Ngwenya, M. P.; Evers, A.; Wade, P. W.; Boeyens, J. C. A.; Dobson, S. M. *Inorg. Chem.* **1990**, *29*, 264.
(11) Mills, D. K. Ph.D. Dissertation, Texas A&M University, 1991.

0020-1669/92/1331-4965$03.00/0

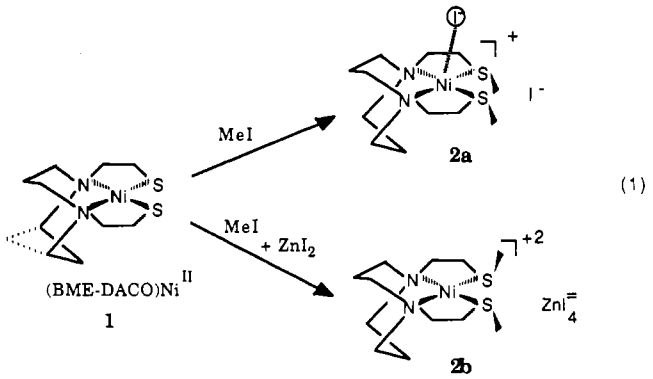

The structure of **2a** suggested that the (BME-DACO)Ni^{II} complex should be a suitable candidate for template syntheses.[12] Thus reactions with 1,3-dibromopropane and bis(2-iodoethyl) ether lead, with good yields, to the formation of new complexes containing macrocyclic ligands, (4,8-dithia-1,11-diazabicyclo-[9.3.3]heptadecane)nickel(II) bromide, [Ni(bicycle)]Br_2 (**3a**), and (7-oxa-4,10-dithia-1,13-diazabicyclo[11.3.3]nonadecane)-iodonickel(II) iodide, [Ni(ether)I]I (**4a**), respectively. Their syntheses and structures demonstrating variable coordination modes are reported below. The structure determined for the ether derivative, [Ni(ether)I]BPh_4, furnished the initial example of an exclusive chair/chair DACO–metal configuration.

Experimental Section

General Procedures. Solvents were reagent grade and used as received. Where anhydrous conditions were required, solvents were purified before use according to published procedures.[13] Acetonitrile was distilled once from CaH_2 and twice from P_2O_5 and was freshly distilled from CaH_2 immediately before use. Bis(2-chloroethyl) ether (Fluka), 1,3-dibromopropane (Aldrich or Eastman), sodium iodide, $NaBH_4$, $NaBF_4$, and $NaBPh_4$ (reagent grade from commercial sources) were used as received. NMR solvents were purchased in sealed ampules from Cambridge Isotope Laboratories and used as received. Where anaerobic conditions were required, standard Schlenk techniques using (Airco) nitrogen or argon (passed through a drying tube of $CaSO_4$, molecular sieves, and NaOH) and an argon glovebox (Vacuum Atmospheres) were employed.

NMR spectra were recorded on a Varian XL-200 FT-NMR spectrometer. Cyclic voltammograms were recorded on a BAS-100A electrochemical analyzer using $Ag^0/AgNO_3$ reference and Pt^0 working electrodes with 0.1 M tetra-*n*-butylammonium hexafluorophosphate in CH_3CN or $Ag^0/AgCl$ reference and glassy carbon working electrodes with 0.1 M KCl in aqueous solutions. EPR data on frozen solutions were obtained at 77 K on a Bruker ESP 300 spectrometer equipped with an Oxford Instruments ER910A cryostat. Elemental analyses were carried out by Galbraith Laboratories, Knoxville, TN. Magnetic susceptibility measurements were performed on an Evans balance purchased from the Johnson Matthey Co. X-ray crystallographic data were obtained on a Nicolet R3m/V single-crystal X-ray diffractometer.

Conductivity measurements were performed using a YSI Model 35 conductance meter equipped with a Barnstead B-1 model E 3411 conductivity bridge (manufactured by Sybron Corp.). Using 0.02 M KCl ($K = 0.002\ 768$ mho cm^{-1}) and the relation $K = L\theta$, the cell constant θ was determined to be 0.112 cm^{-1}. Three freshly distilled portions of CH_3CN were found to have conductivities of ($\times 10^6$ mhos) 1.95, 1.60, and 1.88, well within acceptable limits of pure, dry CH_3CN.

Syntheses. (BME-DACO)Ni^{II} was synthesized according to the published procedure.[9]

(4,8-Dithia-1,11-diazabicyclo[9.3.3]heptadecane)nickel(II) Bromide (3a) or [Ni(bicycle)]Br_2. (BME-DACO)Ni (0.2 g, 0.69 mmol) was dissolved in 20 mL of CH_3CN in a 50-mL Erlenmeyer flask. 1,3-Dibromopropane (1 mL, 1.99 g, 10 mmol) was added rapidly dropwise, and after brief mixing, the flask was stoppered and allowed to stand undisturbed. A portion of the product crystallized overnight, and the color shifted slightly from purple to red/purple along with formation of a small amount of finely divided pale brown solid. With gentle swirling this byproduct was decanted from the crystalline first crop that totaled 0.20 g. Treating the filtered mother liquor with ether gave an additional 0.08 g of product for a total yield of 83% based on (BME-DACO)Ni. If the ether/Ni^{2+} mixture was stirred, or ambient humidity was excessive, the product oiled before dryness was reached. In this case, precipitation with ether was carried out in a Schlenk flask, the supernatant was removed by cannula, and the residues were dried under vacuum. X-ray-quality crystals were obtained from MeOH–CH_3CN/ether. Anal. Calcd (found) for $C_{13}H_{26}N_2S_2Br_2Ni$: C, 31.67 (31.70); H, 5.32 (5.56); N, 5.68 (5.67). ^1H NMR (D_2O) δ (ppm): 1.7 (q, 1.3H), 2.1 (t, 2.4H), 2.7 (t, 3H), 3.0 (t, 3H), 3.25 (q, 4H), 3.6 (t, 8H), 4.5 (br, 2.3H). All signals in the ^1H NMR spectrum were broad and not very well resolved. ^{13}C NMR (D_2O) δ (ppm): 23.0, 25.8, 34.2, 34.4, 53.9, 57.0, 62.2.

(7-Oxa-4,10-dithia-1,13-diazabicyclo[11.3.3]nonadecane)iodonickel-(II) Iodide (4a) or [Ni(ether)I]I and [Ni(ether)I]BPh_4] (4b). The ligand precursor bis(2-iodoethyl) ether was obtained by conversion of the corresponding dichloride using NaI in refluxing acetone.[14] Reaction of 0.1 g (0.34 mmol) of (BME-DACO)Ni in 15 mL of CH_3CN with 0.2 mL (0.392 g, 1.2 mmol) of the iodoether caused a series of color changes culminating in the formation of the green product after standing ca. 3 days. (Note: Use of **1** purified by silica chromatography shortens the reaction time to 1 day). Addition of 100 mL of dry ether to this acetonitrile solution caused the immediate precipitation of the product as a microcrystalline olive-green to brown solid; reversing this order of addition (i.e. adding the complex to ether) causes precipitation, but of a more finely divided product. The supernatant (from which a small second crop was obtained) was removed by cannula and the solid dried under vacuum. The product was moderately hygroscopic, and manipulations were carried out in the glovebox to avoid hydration. Yield: 0.13–0.17 g (62–81%). Crystals suitable for single-crystal X-ray analysis precipitated upon addition of a small amount of $NaBPh_4$ to an acetonitrile solution of the nickel diiodide. Anal. Found (calcd) for $C_{38}H_{48}BIN_2NiOS_2$ (**4b**): C, 56.08 (56.39); H, 6.06 (5.98); O, 1.37 (1.98). Mp: 238 °C dec. With the exception of the hygroscopic nature of **4a**, both species were air stable. Bromo and chloro derivatives of complex **4** were similarly prepared using the appropriate $XCH_2CH_2OCH_2CH_2X$ compound.

Ion Exchanges. The dibromide salt of **3** was treated with $AgBF_4$ in methanol, precipitating AgBr, which was isolated by filtration. The ion-exchanged product [Ni(bicycle)]$[BF_4]_2$ (**3b**) was obtained as a red microcrystalline solid after solvent evaporation. Ion exchanges of the counterion of **4** were accomplished in CH_3CN with $NaBPh_4$ or $NaBF_4$, with stirring overnight, resulting in precipitation of NaX. The solution was filtered through Celite and the final product obtained by solvent evaporation. Removal of the nickel-bound halide required aqueous solution. Thus [Ni(ether)I]I dissolved in water (yielding a pink solution) was treated with 2 equiv of $NaBPh_4$. The pink precipitate formed was washed three times with water and then with ether.

Reduction of [Ni(bicycle)]Br_2 and [Ni(ether)I]I with $NaBH_4$. Under anaerobic conditions, a 50-mL Schlenk flask was charged with ca. 0.1 g of the nickel complex and then with 10 mL of dry CH_3CN. In the case of **3a**, a slight molar excess of the 0.10 M $NaBH_4$ stock solution was added and after ca. 20 min the color shifted from violet to brown. A sample for EPR analysis was prepared from the solution obtained after filtration through Celite and stored at −196 °C.

To reduce **4a**, ca. 2.5 equiv of $NaBH_4$ was used. The mixture was gently heated in an oil bath to 65–70 °C under N_2 for 4 days, during which time the color changed from green to golden yellow. A sample for EPR analysis was obtained as described above.

X-ray Crystal Structure Determination. Collection and Reduction of X-ray Data. Crystals for structural analysis of **3a** (purple block) and **4b** (emerald green parallelepiped) were mounted on a glass fiber with epoxy cement, at room temperature. Cell parameters (see Table I) were calculated from the least-squares fitting of the setting angles for 25 reflections ($2\theta_{av} = 19.4$). ω scans for several intense reflections indicated acceptable crystal quality. Data were collected for $4.0° \le 2\theta \le 50.0°$ [ω(Wyckoff) scans] at 296 K. Scan widths on ω, for the data collection were 1.20° plus Kα separation with a variable scan rate of 1.50–14.65° min^{-1} for **3a** and 1.20° with a variable scan rate of 2.00–15.00° min^{-1} for **4b**. Three control reflections, collected every 97 reflections, showed no significant trends. Lorentz and polarization corrections were applied

(12) Thompson, M. C.; Busch, D. H. *J. Am. Chem. Soc.* **1964**, *86*, 3651.
(13) Gordon, A. J.; Ford, R. A. *The Chemist's Companion*; Wiley and Sons: New York, 1972; pp 429–436.
(14) Kulstad, S.; Malmsten, L. Å. *Acta Chem. Scand.* **1979**, *B33*, 469.

to 7508 and 3556 reflections for **3a** and **4b**, respectively. Semiempirical[15] absorption corrections were applied (ellipsoid approximation; for bicycle $\mu r = 0.05$, $T_{max} = 0.9933$, $T_{min} = 0.6731$; for ether $\mu r = 0.10$; $T_{max} = 0.968$, $T_{min} = 0.737$). A total of 2711 unique reflections ($R_{int} = 0.03$),[16] with $|I| \geq 3.0\sigma(I)$, were used in further calculations for **3a**, whereas the 3556 unique reflections were used in calculations for **4b**.

Solution and Refinement. The molecular structures were solved by direct methods[15] and refined anisotropically for all non-hydrogen atoms with full-matrix least-squares methods [quantity minimized $\sum w(F_o - F_c)^2$, where $w^{-1} = \sigma^2(F) + gF^2$]. For **3a**, the number of least-squares parameters used was 398, $R = 0.043$, $R_w = 0.038$, and $S = 1.16$ at convergence[16] [largest $\Delta/\sigma = 0.2750$; mean $\Delta/\sigma = 0.0280$; largest positive peak in the final Fourier difference map = 0.74 e Å^{-3}; largest negative peak in the final Fourier difference map = –0.56 e Å^{-3}]. For **4b**, the number of least-squares parameters used was 417, $R = 0.039$, $R_w = 0.047$, and $S = 1.07$ at convergence[16] [largest $\Delta/\sigma = 0.0009$; mean $\Delta/\sigma = 0.0002$; largest positive peak in the final Fourier difference map = 0.41 e Å^{-3}; largest negative peak in the final Fourier difference map = –0.62 e Å^{-3}]. For **4b**, the Rodgers absolute configuration parameter η was refined to 1.13 (5) and a Hamilton significance test indicated that the correct absolute configuration was chosen.[17]

The extinction coefficient χ {where $F^* = F_c/[1 + 0.002\chi F_c^2/\sin(2\theta)]^{0.25}$} was refined 0.000 17 (5) for **4b**.[18] For both complexes, hydrogen atoms were placed in idealized positions with isotropic thermal parameters fixed at 0.08. Neutral-atom scattering factors and anomalous scattering correction terms were taken from a standard source.[19]

Results

Synthesis and Characterization. The complexes [Ni(bicycle)]Br_2 (**3a**) and [Ni(ether)I]I (**4a**) were obtained in the reaction of (BME-DACO)Ni with 1,3-dibromopropane and bis(2-iodoethyl) ether, respectively (eq 2). For **4**, eq 2 also displays the products

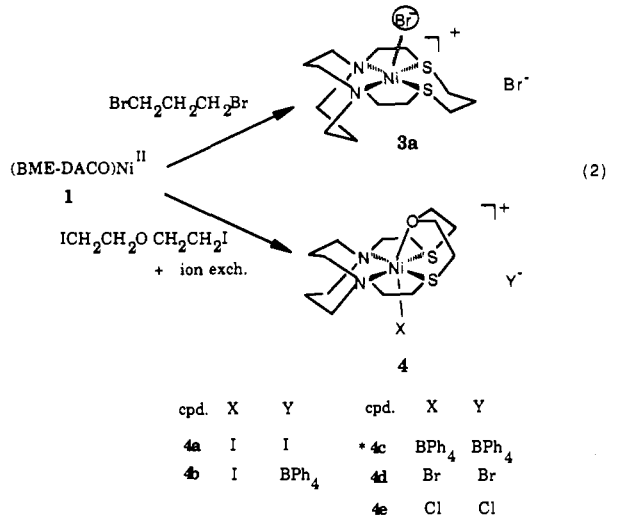

cpd.	X	Y	cpd.	X	Y
4a	I	I	* **4c**	BPh_4	BPh_4
4b	I	BPh_4	**4d**	Br	Br
			4e	Cl	Cl

* Structural change. See text.

obtained through ion exchange and their designations. Compound **3b** is [Ni(bicycle)][BF_4]$_2$. The exceptionally good yields of ring-closed products, maximized to over 80%, attest to the template effect of the immobilized thiolate sulfurs.[12] This, combined with the steric bulk of the DACO backbone, hinders the formation of the intractable polymers observed in complexes with less sterically demanding ligands such as 2-aminoethanethiol.[12]

Table I. Experimental Data for the X-ray Crystal Structures of [Ni(bicycle)]$Br_2 \cdot 2H_2O$ (**3a**) and [Ni(ether)I]BPh_4 (**4b**)

	3a	**4b**
chem formula	$C_{13}H_{30}N_2O_2S_2NiBr_2$	$C_{38}H_{48}N_2OS_2NiIB$
fw	529.0	809.3
space group	monoclinic $P2_1/c$ (No. 14)	orthorhombic $P2_12_12_1$ (No. 18)
a, Å	17.384 (7)	10.016 (2)
b, Å	15.529 (6)	11.834 (3)
c, Å	15.153 (4)	30.127 (8)
β, deg	104.42 (3)	
V, Å^3	3962 (2)	3570 (1)
Z	8	4
ρ(calcd), g cm^{-3}	1.774	1.505
temp, °C	23	23
radiation (λ, Å)	Mo Kα (0.710 73)	Mo Kα (0.710 73)
abs coeff, mm^{-1}	5.191	1.545
min/max transm coeff	0.6731/0.9933	0.737/0.968
R,[a] %	4.3	3.9
R_w,[a] %	3.8	4.7

[a] Residuals: $R = \sum|F_o - F_c|/\sum F_o$; $R_w = \{[\sum w(F_o - F_c)^2]/[\sum w(F_o)^2]\}^{1/2}$.

Both types of complexes can be demetalated by the reaction with excess CN^-, rendering free ligands in the form of yellowish oils upon extraction and solvent removal. The complexes were reconstituted on addition of nickel(II) bromide.

Certain physical and spectroscopic properties of these complexes are listed in Table II. Molar conductivity measurements in acetonitrile find **3a**, **4a**, and **4d** to be uni-univalent electrolytes, whereas **4c** and **3b** are di-univalent electrolytes.[20]

The colors and spectral properties of the macrocyclic complexes corroborate the coordination numbers/geometries suggested from the magnetism and conductivity data. Purple crystals of **3a** dissolve in CH_3CN to give a violet solution, characterized by two bands in the visible region (Table II) and an intense charge-transfer absorption between 200 and 400 nm. Similar patterns, typically associated with the $\nu_2(^3A_{2g} \rightarrow {}^3T_{1g})$ and $\nu_3(^3A_{2g} \rightarrow {}^3T_{1g}(P))$ transitions in six-coordinate, pseudooctahedral Ni^{II} complexes,[21] are observed for the green CH_3CN solutions of compounds **4a** and **4d**. If [Ni(bicycle)Br]Br is indeed hexacoordinate in CH_3CN solution, the sixth coordination site must be taken by a solvent molecule, rather than a second bromide anion, since the conductivity data find such solutions to contain uni-univalent electrolytes. Water solutions of **3a**, as well as CH_3CN solutions of **3b**, are red and have a single band in the visible region at ca. 485 nm, characteristic of four-coordinate, square-planar Ni^{II} complexes.[22,23] Complex **4c**, which has halides completely exchanged by BPh_4^- anions, is pink in CH_3CN solution, displays only one band, and is assumed to similarly be square planar in solution. Complex **4c** is insoluble in water; however **4a** and **4d** dissolve, yielding pink solutions with a weak single band in the visible region, characteristic of square-planar compounds.

Acetonitrile solutions of the six-coordinate ether complexes **4a** and **4d** show molar extinction coefficients to dramatically increase with the size of the halide, Br < I. This observation is consistent with the polarizability and ligand field strengths of the halides and further indicates that they are present in the first coordination sphere of Ni.[24] The slight shift toward the red on changing from

(15) All crystallographic calculations were performed on a μVaxII minicomputer with SHELXTL-PLUS, revision 4.3 (G. M. Sheldrick, Institut für Anorganische Chemie der Universität, Tammannstrasse 4, D-3400 Göttingen, Germany), supplied by Siemens Analytical X-ray Instruments, Madison, WI.

(16) Residuals: $R_{int} = [\sum F^2 - (F_{mean})^2]/[\sum F^2]$; $R = \sum|F_o - F_c|/\sum F_o$; $R_w = \{[\sum w(F_o - F_c)^2]/[\sum w(F_o)^2]\}^{1/2}$; $S = \{[\sum w(F_o - F_c)^2/[N_{data} - N_{params}]\}^{1/2}$.

(17) Rodgers, D. *Acta Crystallogr.* **1981**, *A37*, 734. Jones, P. G. *Acta Crystallogr.* **1984**, *A40*, 660. Hamilton significance test: Hamilton, W. C. *Acta Crystallogr.* **1965**, *17*, 502.

(18) Larson, A. C. *Acta Crystallogr.* **1967**, *A23*, 604.

(19) *International Tables for X-Ray Crystallography*; Ibers, J. A., Hamilton, W. C., Eds.; Kynoch Press: Birmingham, England, 1974; Vol. 4, pp 99, 149.

(20) Figgis, B. N.; Lewis, J. In *Modern Coordination Chemistry. Principles and Methods*; Lewis, J., Wilkins, R. G., Eds.; Interscience Publishers Inc.: New York, 1960; p 400.

(21) Busch, D. H.; Jicha, D. C.; Thompson, M. C.; Wrathal, J. W.; Blinn, E. *J. Am. Chem. Soc.* **1964**, *86*, 3642.

(22) Billo, E. J. *Inorg. Chim. Acta* **1979**, *37*, L533.

(23) Lever, A. B. P. *Inorganic Electronic Spectroscopy*, 2nd ed.; Elsevier: Amsterdam, 1984.

(24) Workman, M. O.; Dyer, G.; Meek, D. W. *Inorg. Chem.* **1967**, *6*, 1543.

Table II. Physical/Spectroscopic Data for [Ni(bicycle)]X_2, [Ni(ether)X]Y, and [Ni(ether)]Y_2 Complexes

complex	no.	color solid/CH_3CN/H_2O	μ_{eff},[a] μ_B (20 °C)	Λ_M,[b] cm^2 Ω^{-1} mol^{-1}	UV–vis λ, nm (ε) acetonitrile	water
[Ni(bicycle)]Br_2	**3a**	purple/violet/red	diam[c]	145	410 (151), 581 (142)	484 (287)
[Ni(bicycle)][BF_4]$_2$	**3b**	red/red/red	diam	318	488 (275)	
[Ni(ether)I]I	**4a**	olive-green/green/pink	1.86	157	431 (1046), 651 (112)	499 (93)
[Ni(ether)Br]Br	**4d**	green/green/pink	2.66	138	417 (171), 640 (67)	470 (166)
[Ni(ether)][BPh_4]$_2$	**4c**	pink/pink/insoluble	diam	251	472 (139)	

[a] Solid-state measurements. [b] Molar conductance values for ca. 10^{-3} M solutions of the compounds in acetonitrile. [c] Diamagnetic in solid state; in CD_3CN/CD_3OD (70/30) μ_{eff} = 2.21 μ_B (Evans' NMR method).

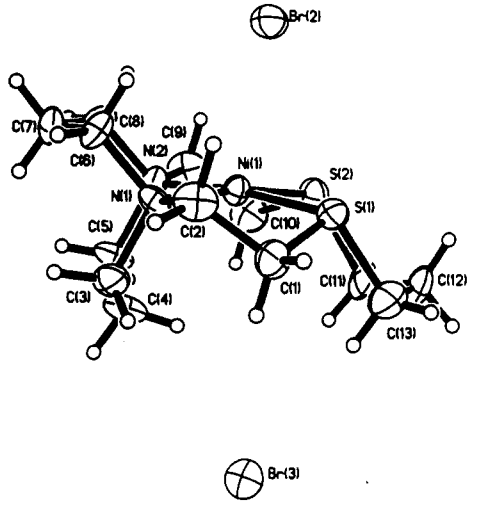

Figure 1. Molecular structure of [Ni(bicycle)]Br_2 (**3a**) showing the atom-labeling scheme (thermal ellipsoid plot at 50% probability).

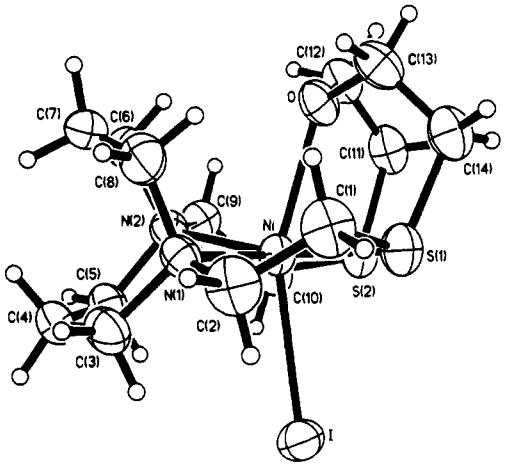

Figure 2. Molecular structure of the cationic portion of [Ni(ether)I]-BPh_4 (**4b**) with the atom-labeling scheme (thermal ellipsoid plot at 50% probability).

bromo to iodo ligands was previously observed in the aminoethyl thioether complexes of nickel.[21,24]

X-ray Structures. The molecular structures of **3a** and **4b** are shown in Figures 1 and 2, respectively, and selected bond lengths and bond angles are listed in Table III. Full listings of bond lengths and bond angles, packing diagrams, and lists of anisotropic displacement coefficients for both complexes are available as supplementary material.

Complex **3a** (Figure 1) crystallizes in the monoclinic crystal system with two complexes and four water molecules in the asymmetric unit. The nickel ion is in an almost ideal square-planar environment in this complex and is involved in three six-membered metalla rings. Those derived from the DACO portion of the ligand are in chair and boat configurations, and the additional sulfur-containing ring is in the chair configuration. The Ni–N_{av} and Ni–S_{av} distances of 1.985 and 2.195 Å, respectively, are almost identical with those in the acyclic complexes **2a** and **2b**.[9,11] One bromide ion is distributed through the lattice as a counterion; a second is positioned over the more open side of the NiN_2S_2 plane. This bromide anion is 2.947 (2) Å from nickel, ca. 0.5 Å farther than the average literature values of Ni–Br bond distances, 2.41 Å.[25] Despite such a large distance, the angles formed by bromide, nickel, and the donor atoms in the NiN_2S_2 square plane indicate that bromide's position as a long-range axial ligand in a square pyramid is quite regular. The pendant arms (CH_2CH_2S) in **3a** are eclipsed. As was observed for the DACODA complexes of Ni and Co,[6,7] the central methylene C–H group of the boat form of the metalladiazacyclohexane ring shields the metal center in **3a** with a H–Ni distance of 2.601 (5) Å.

Table III. Selected Bond Lengths (Å)[a] and Bond Angles (deg)[a] for [Ni(bicycle)]Br_2·$2H_2O$ (**3a**) and [Ni(ether)I]BPh_4 (**4b**)

	[Ni(bicycle)]Br_2·$2H_2O$	[Ni(ether)I]BPh_4
	Bond Lengths	
Ni(1)–S(1)	2.201 (3)	2.405 (2)
Ni(1)–S(2)	2.188 (3)	2.362 (2)
Ni(1)–N(1)	1.990 (7)	2.101 (5)
Ni(1)–N(2)	1.983 (8)	2.116 (5)
Ni(1)–X[b]	2.947 (2)	2.814 (1)
Ni(1)–O		2.387 (5)
	Bond Angles	
N(1)–Ni(1)–N(2)	89.2 (3)	85.5 (2)
S(1)–Ni(1)–S(2)	89.9 (1)	97.4 (1)
S(1)–Ni(1)–N(1)	90.2 (2)	87.7 (1)
S(1)–Ni(1)–N(2)	173.5 (3)	165.6 (1)
S(2)–Ni(1)–N(1)	172.7 (3)	174.8 (1)
S(2)–Ni(1)–N(2)	89.8 (2)	89.8 (1)
X[b]–Ni(1)–S(1)	87.9 (1)	88.7 (1)
X[b]–Ni(1)–S(2)	89.7 (1)	82.5 (1)
X[b]–Ni(1)–N(1)	97.6 (3)	96.6 (1)
X[b]–Ni(1)–N(2)	98.7 (3)	104.2 (1)
O–Ni(1)–S(1)		79.3 (1)
O–Ni(1)–S(2)		78.5 (1)
O–Ni(1)–N(1)		103.7 (2)
O–Ni(1)–N(2)		90.0 (2)
O–Ni(1)–X[b]		155.8 (1)

[a] Estimated standard deviations are given in parentheses. [b] X = Br(2) in complex **3a**; X = I in complex **4b**.

Complex **4b** (Figure 2) uses the additional ether donor site to generate six-coordinate nickel in a distorted octahedral environment. The N_2S_2 equatorial donor set also shows deviation from planarity; the N(2)–Ni–S(1) angle is 165.6 (1)°, and one sulfur atom lies 0.58 Å off the N_2SNi plane. The axial ligands, sterically restrained by the DACO ring from a more perpendicular approach to the metal, are not linear; the I–Ni–O bond angle is 155.8 (1)°. Further, one of the hydrogens on the ether linkage α to the oxygen has a near contact of 2.160 Å with a hydrogen on the carbon (α to the nitrogen) of the ethyl pendant arm. In contrast to the bicyclic complex **3a**, the ethanethiolato pentant arms are staggered, as in the starting material (BME-DACO)-Ni.[9] *The most unusual feature in this structure is the chair/chair conformation of the DACO trimethylene rings.*

(25) Orpen, A. G.; Brammer, L.; Allen, F. H.; Kennard, O.; Watson, D. G.; Taylor, R. *J. Chem. Soc., Dalton Trans.* **1989**, S1.

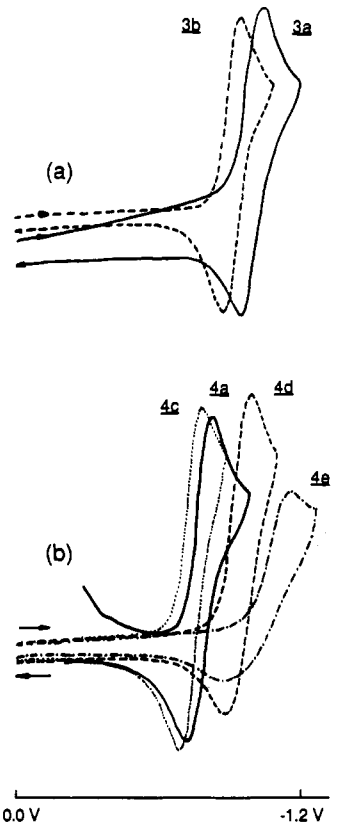

Figure 3. Cyclic voltammograms (ca. 1 mM solutions in acetonitrile; scanned first toward negative potential; scan rate 200 mV/s): (a) (—) [Ni(bicycle)]Br_2 (**3a**), (- - -) [Ni(bicycle)][BF_4]$_2$ (**3b**); (b) (···) [Ni(ether)]-[BPh_4]$_2$ (**4c**), (—) [Ni(ether)I]I (**4a**), (- - -) [Ni(ether)Br]Br (**4d**), (- · -) [Ni(ether)Cl]Cl (**4e**).

The comparison of Ni–donor atom bond lengths found in Table III shows a dramatic increase in macrocyclic cavity size in **4b** as compared with **3a**. The nickel–sulfur distances in the former are ca. 0.2 Å longer than those in the latter, and the Ni–N distances are also longer in **4b** (by 0.1 Å). Discrepancies in bond angles are also seen. The most significant difference is the near 8° increase of ∠S–Ni–S in **4b**, resulting in a S- - -S separation of 3.58 (1) Å (as contrasted to 3.10 (1) Å in **3a**), which is accounted for by the larger sulfur–sulfur bridge. A smaller contraction (ca. 4°) of ∠N–Ni–N accompanies the increase in ∠S–Ni–S.

Electrochemistry. In acetonitrile solution, the [Ni(bicycle)] complexes exhibit reversible $Ni^{II/I}$ redox behavior (Figure 3a), as does [Ni(ether)I]I (Figure 3b). All other derivatives of **4** exhibit quasi-reversible Ni^{II}/Ni^{I} redox couples (Table IV and Figure 3b). The reduction of **4** becomes easier with the change of the halide ligand from chloride to bromide to iodide (Figure 3b). Bulky, noninteracting counterions appear to facilitate the reduction of **4**; however, reversibility is impaired (Table IV). In water, [Ni(ether)I]I and [Ni(ether)Br]Br have the same redox potentials for the $Ni^{II/I}$ process, indicating that the same species is being reduced. Since, in addition, both have the same color in aqueous solution, it is safe to conclude that their coordination modes are the same in H_2O and are different from those in the solid state and in acetonitrile solution. The same holds true for complexes of **3**.

Comparison of [Ni(ether)] and [Ni(bicycle)] derivatives indicates that while the $Ni^{II/I}$ processes of the latter are more reversible, they are also more difficult to achieve (Table IV). Notably this is true both in acetonitrile solution, where the complexes are most likely six-coordinate, and in water, where they are four-coordinate. This feature is ascribed to the difference in the cavity size of the ligands with the larger N_2S_2 cavity of the ether macrocycle accommodating the larger Ni^{I} more comfortably.[26] Not surprisingly, the reduction is easier for both **3** and **4** in H_2O vs CH_3CN.

Table IV. Cyclic Voltammetric Results

compound	$E_{1/2}(Ni^{II/I})$, mV[a]	I_{pa}/I_{pc}	ΔE, mV
Acetonitrile Solutions[b]			
[Ni(ether)I]I (**4a**)	−790	0.73	88
[Ni(ether)I]BPh_4 (**4b**)	−776	0.57	120
[Ni(ether)][BPh_4]$_2$ (**4c**)	−750	0.27	99
[Ni(ether)I]BF_4	−768	0.38	144
[Ni(ether)Br]Br (**4d**)	−930	0.52	140
[Ni(ether)Br]BPh_4	−886	0.34	180
[Ni(ether)Br]BF_4	−903	0.42	162
[Ni(ether)Cl]Cl (**4e**)	−1040	0.80	130
[Ni(bicycle)]Br_2 (**3a**)	−1042	0.79	76
[Ni(bicycle)][BF_4]$_2$ (**3b**)	−968	0.83	72
Water Solutions[c]			
[Ni(bicycle)]Br_2 (**3a**)	−885	1.00	78
[Ni(bicycle)][BF_4]$_2$ (**3b**)	−871	0.76	66
[Ni(ether)I]I (**4a**)	−666	0.88	76
[Ni(ether)Br]Br (**4d**)	−663	0.96	84

[a] All entries referenced to $Ag/AgNO_3$. [b] With Pt vs $Ag/AgNO_3$ electrodes and 0.1 M [*n*-Bu_4N]PF_6 as supporting electrolyte; scan rate 200 mV/s. [c] With glassy carbon vs Ag/AgCl electrodes, 0.1 M KCl as supporting electrolyte, and scan rate 200 mV/s, the redox potentials in aqueous solutions were as follows (mV): **3a**, −855; **3b**, −841; **4a**, −636; **4d**, −633. A factor of 30 mV corrects for the difference in reference electrodes as measured by the first reduction potential of methyl viologen dichloride in water and in acetonitrile solution: $E_{1/2}(H_2O)$ = −699 mV; $E_{1/2}(CH_3CN)$ = −729 mV.

Supporting evidence for the formation of Ni^{I} species, i.e., a metal-based reduction, was provided by the observation of EPR signals detected on frozen (−196 °C) solution samples of **3a** and **4a**, chemically reduced by $NaBH_4$. Both EPR spectra demonstrated axial signals typical of d^9 systems, with $g_{\parallel} > g_{\perp}$.[26] For reduced **3a**, the EPR analysis gave $g_{\parallel}$ = 2.20 and $g_{\perp}$ = 2.06, while reduced **4a** gave $g_{\parallel}$ = 2.24 and $g_{\perp}$ = 2.06.

Discussion

Chart II summarizes the conditions which control coordination numbers/geometries of the macrocyclic N_2S_2 nickel complexes delineated in this study and provides further examples of the delicate balance of factors that direct six-coordinate, high-spin nickel to convert to four-coordinate, low-spin nickel. Of all the complexes reported here, the most obvious structural analogues are the four-coordinate square-planar geometries found when salts of complexes **3** and **4** are dissolved in water. The square-planar form is promoted by good anion solvation, the poor donor ability of water, and, as well, the hydrophobic character and steric restrictions of the hydrocarbon substituents attached to the S and N donor sites. Square-planar forms are also observed for acetonitrile solutions of both **3** and **4** containing bulky, noncoordinating counterions, e.g., BF_4^- and BPh_4^-.

The coordination environment of [Ni(ether)X]$^+$ derivatives in acetonitrile solutions is arguable due to the possibility that the oxygen donor atom could be displaced by acetonitrile. We were unable to obtain solid-state spectra of sufficient quality to relate to the acetonitrile solution spectrum of **4a**. However, when dissolved in methylene chloride, **4a** gave a two-band spectrum very similar to that obtained in acetonitrile (CH_2Cl_2: λ = 434 nm, ε = 429; λ = 660 nm, ε = 43). Since the typically noncoordinating solvent CH_2Cl_2 should not displace the ether oxygen donor, we conclude from the spectral similarity that CH_3CN likewise does not substitute for the O donor atom in solution.

Noteworthy is the fact that the ether donor site of **4** is utilized only in acetonitrile *when a halide is present as a sixth ligand.* Removal of the halide and substitution by bulky counterions effect

(26) Lovecchio, F. V.; Gore, E. S.; Busch, D. H. *J. Am. Chem. Soc.* **1974**, *96*, 3109.

Chart II

Forms of the Macrocycle Ni Compounds

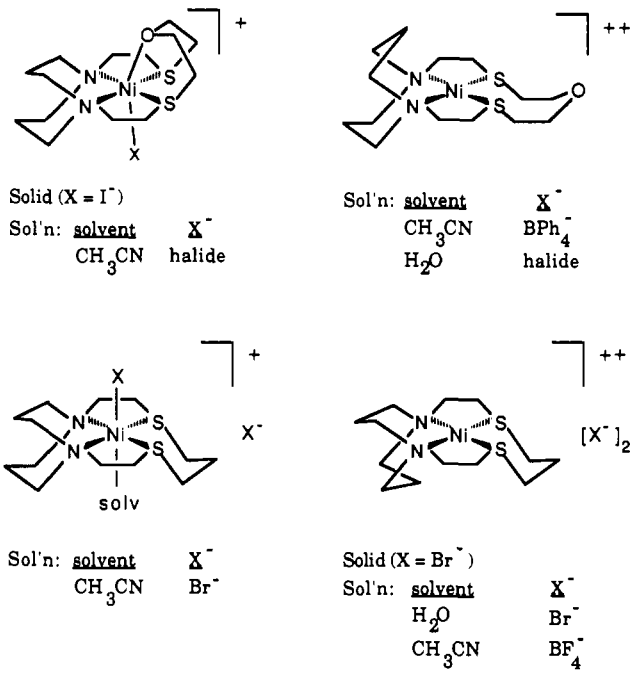

Chart III

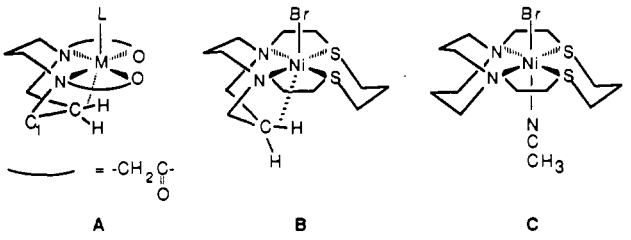

release of the O-donor site, resulting in square-planar, four-coordinate complexes.

Nevertheless, acetonitrile is reported to coordinate to metals in related nickel–thioether complexes,[27] and thus questions about the assumed structure of **3a** in acetonitrile arise. The representation of **3a** in Chart II as a pseudooctahedral complex with acetonitrile as the sixth ligand is tentative and based on similarities of its electronic spectrum with those of the octahedral complexes **4a** and **4d**. In fact, the pentacoordinate, distorted square-pyramidal form of (DACODA)$(SO_3)Co^{III}$ in the solid state and in solution gives UV–vis spectra typical of octahedral Co^{III} complexes.[7] As discussed by Legg et al.[7] and indicated by structure A (Chart III), an agostic C–H interaction (Co–H = 2.31 (5) Å) from the boat form of the metalladiazacyclohexane ring is effectively the sixth "ligand". Therefore, the possibility exists that the two-band pattern in the UV–vis spectrum of **3a** might reflect pseudooctahedral geometry with one bound bromide and an agostic C–H perturbing the site trans to Br^-, structure B (Chart III). However, a similarly strong agostic interaction for Ni^{II} is contraindicated by the two electrons in the d_{z^2} orbital of Ni^{II} leading in compound **3a** to a Ni–H distance of 2.60 Å. In (DACODA)(H_2O)Ni, the analogous Ni–H distance is 2.51 (9) Å.[6a] As was also pointed out by Legg et al.,[7] a further indication of the agostic interaction in the Co^{III} complex is the degree of strain in the metalladiazacyclohexane ring. While the M–N–C(1) angle in structure A for M = Co and L = SO_3 is 100.7 (3)°, it is 106.7 (6)° for M = Ni and L = H_2O.[7] In the solid-state structure of compound **3a** (Figure 1), the analogous angle is 107.8 (5) Å. It is thus unlikely that a β-methylene C–H interaction is even present or sufficiently strong to account for the spectral similarities with octahedral complexes. On the other hand, our results clearly show that the metalladiazacyclohexane rings may assume chair/chair forms, as they do in **4b**, thus alleviating the steric hindrance associated with axial ligation and permitting six-coordinate, high-spin Ni^{II} complexes on addition of a strongly binding sixth ligand. Such a scenario is represented as structure C for the solution-state structure of **3a**. The DACO ligand therefore may be used as a steric restrictor of axial ligation only with caution. There is certainly no straightforward evidence that any of the complexes reported here, despite being primed for such, in fact demonstrate square-pyramidal coordination geometries.

The factors which determine coordination numbers in Ni^{II} complexes have long been recognized as complicated.[28-30] The pentacoordination discussed above for the (DACODA)(H_2O)-Ni^{II} compound results from the hard N_2O_2 donor sites of the chelate ligand which are expected to render Ni^{II} "hard" and susceptible to axial ligation. The sixth position is blocked by the boat form of the DACO ring. However, should a more strongly binding ligand be offered to Ni^{II}, our results suggest six-coordination involving chair/chair forms would be possible. On the other hand, the definitely "soft" P_2S_2 donor sites of the pssp ligand ($Ph_2PCH_2CH_2SCH_2CH_2CH_2SCH_2CH_2PPh_2$) also allow for the accommodation of a fifth ligand in the Br–Ni(pssp)$^+$ complex (Ni–Br = 2.645 (4) Å)[31] and in organometallic derivatives of that complex.[32] Hence, there is no reason to expect that the mixed hard/soft environment of the N_2S_2Ni complexes will rule out pentacoordination. A prudent conclusion regarding the geometry about Ni in acetonitrile solutions of **3a** is as follows. Spectral features are best explained by the usual octahedral geometry; however, if classically pentacoordinate square-pyramidal geometry obtains, the spectral features are little distinguished from octahedral complexes such as **4a**.

The structure of [Ni(ether)I]BPh_4 is to our knowledge the first report of a metal complex derivative of DACO with the chair/chair conformation and sparks new controversy on the factors which control the conformation of the ligand. Intuitively, the energy gained from the formation of the two axial bonds must compensate for the unfavored steric repulsions of the DACO ring. Interestingly, MM2 calculations[33] carried out for complex **2b** find only small differences between the two lowest energy forms of the DACO portion of the BME-DACO ligand, the chair/chair and the boat/chair forms; however, *the lower energy form is that with the chair/chair configuration*, the one seen for **4b**. These results agree with earlier MM calculations on $(DACO)_2Ni^{2+}$ and the observation, based on NMR results, of a low barrier for ring inversion in that complex.[34] Also shown by our calculations on **2b**, which include the metal with non-zero dihedral energies, is that the strain in the DACO ring has a much stronger influence on the energy of the system than does the eclipsed or staggered orientation of the pendant arms.

(27) Cha, M.; Kovacs, J. A. *Abstracts of Papers*, 201st National Meeting of the American Chemical Society, Atlanta, GA, April 14–19, 1991; American Chemical Society: Washington, DC, 1991.

(28) Busch, D. H. *Adv. Chem. Ser.* **1966**, *40*, 616.
(29) Martell, A. E.; Calvin, M. *Chemistry of the Metal Chelate Compounds*; Prentice Hall, Inc.: New York, 1952.
(30) Lifschitz, I.; Bos, J. G.; Dijkema, K. M. *Z. Anorg. Allg. Chem.* **1939**, *242*, 97.
(31) Bertinsson, G.-I. *Acta Crystallogr.* **1983**, *C39*, 698.
(32) Chojnacki, S.; Darensbourg, M. Y.; Hinton, P.; Hsiao, Y. M.; Kim, J. S.; Reibenspeis, J. H. Unpublished results.
(33) MM2 calculations (Berkert, U.; Allinger, N. L. *ACS Monogr.* **1982**, *177*) were undertaken employing the program MacroModel 3.0 (Clark Still, Columbia University, New York, 1990) and the block diagonal Newton Raphson minimization technique. MM2 parameters for the Ni atom were taken from known structural and physical properties (Hopfinger, A. J.; Pearlstein, R. A. *J. Comput. Chem.* **1984**, *5*, 486).
(34) Sardella, D. J.; Billo, E. J.; Connolly, P. J. *Inorg. Chim. Acta* **1988**, *142*, 119.

Despite the steric repulsion of hydrogens on the β-carbons of the DACO backbone in the chair/chair configuration (in **4b** those hydrogens are only 1.735 Å apart), the usual stereochemical preference of cyclohexane rings appears to hold in the metalladiazacyclohexane. Hence we conclude by questioning the predominance of chair/boat forms of DACO in the complexes thus far studied, rather than the appearance of the chair/chair form in cases of the original parent complex **1**, the octahedral complex **4b**, and other six-coordinate derivatives.[35]

Acknowledgment. The National Institutes of Health is acknowledged for funding of this work (Grant RO1 GM44865-01) and the National Science Foundation for the X-ray diffractometer and crystallographic computing system (Grant CHE-8513273) as well as the EPR spectrometer (Grant NSF CHE-8912763). The authors express appreciation to Prof. Paul Lindahl and Mr. Patrick J. Farmer for their help.

(35) Goodman, D. C.; Tuntalani, T.; Farmer, P. J.; Darensbourg, M. Y.; Reibenspies, J. H. *Angew. Chem.*, in press.

Supplementary Material Available: Tables of crystallographic data collection parameters and atomic coordinates and equivalent isotropic displacement parameters, complete listings of bond lengths and bond angles, anisotropic displacement parameters, and H atom coordinates and isotropic displacement parameters for **3a** and **4b**, an ORTEP drawing of the BPh_4^- anion of **4b**, and packing diagrams of **3a** and **4b** (15 pages). Ordering information is given on any current masthead page.